http://dx.doi.org/10.5012/bkcs.2012.33.8.2546

Biguanide-Functionalized Fe_3O_4/SiO_2 Magnetic Nanoparticles: An Efficient Heterogeneous Organosuperbase Catalyst for Various Organic Transformations in Aqueous Media

Abdolhamid Alizadeh,[†,‡,*] Mohammad M. Khodaei,[†,‡,*] Mojtaba Beygzadeh,[†] Davood Kordestani,[†] and Mostafa Feyzi[†]

[†]*Faculty of Chemistry, Department of Organic Chemistry, Razi University, Kermanshah 67149, Iran*
[‡]*Nanoscience & Nanotechnology Research Center (NNRC), Razi University, Kermanshah 67149, Iran*
[*]*E-mail: ahalizadeh2@hotmail.com (A. A.); mmkhoda@razi.ac.ir (M. M. K)*
Received March 19, 2012, Accepted May 3, 2012

A novel biguanide-functionalized Fe_3O_4/SiO_2 magnetite nanoparticle with a core-shell structure was developed for utilization as a heterogeneous organosuperbase in chemical transformations. The structural, surface, and magnetic characteristics of the nanosized catalyst were investigated by various techniques such as transmission electron microscopy (TEM), powder X-ray diffraction (XRD), vibrating sample magnetometry (VSM), elemental analyzer (EA), thermogravimetric analysis (TGA), N_2 adsorption-desorption (BET and BJH) and FT-IR. The biguanide-functionalized Fe_3O_4/SiO_2 nanoparticles showed a superpara-magnetic property with a saturation magnetization value of 46.7 emu/g, indicating great potential for application in magnetically separation technologies. In application point of view, the prepared catalyst was found to act as an efficient recoverable nanocatalyst in nitroaldol and domino Knoevenagel condensation/Michael addition/cyclization reactions in aqueous media under mild condition. Additionally, the catalyst was reused six times without significant degradation in catalytic activity and performance.

Key Words : Magnetic nanoparticles, Interfacial catalysts, Surface-modification, Organosuperbases

Introduction

Organosuperbases such as amidines, guanidines and biguanides (Scheme 1) have attracted much attention in synthetic organic chemistry and are known as "proton sponges".[1] Biguanides that contain three amino groups are stronger than amines, amidines, guanidines. They can be considered as a new class of strong super-basic organocatalyst in various chemical transformations.[2] The recovery of these kind of catalysts is difficult and their utilization is associated with environmental pollution.

Heterogenation of the existing homogeneous organosuperbase catalyst could be an attractive solution to this problem because the heterogeneous catalysts can be easily separated from the reaction mixture.[3,4] Most of supported catalysts are separated by filtration or centrifugation. In contrast, Fe_3O_4-supported catalysts can be easily separated from the reaction mixture by an external permanent magnet.[5-8]

Over the last years, several solid surface-immobilized catalysts such as aminoalkylsilane-functionalized silica,[9] guanidine-immobilized SBA-15, amino-functionalized magnetic nanoparticles and *etc*. have been prepared to efficiently catalyze the chemical transformations.[10,11] A literature survey revealed that despite their promising catalytic applications of biguanides, the preparation of solid-supported biguanide catalysts have not been subjected to detailed investigations In fact, only a 20-years-old study of Gelbard and co-workers has reported the synthesis of polystyrene-supported biguanides and their utilization as catalysts in the transesterification of several vegetal oils.[12] Here, we report a versatile and convenient procedure for synthesizing of a recoverable and reusable Fe_3O_4/SiO_2-supported biguanide nanocatalyst by the direct attachment of a biguanide; namely metformin, on silica-coated Fe_3O_4 nanoparticles through a covalent bond linkage. It has been shown that the catalyst is capable of promoting the various organic transformations such as nitroaldol and domino Knoevenagel condensation/Michael addition/cyclization reactions for the preparation of several organic compounds in a green medium (H_2O/EtOH) instead of traditional hazardous organic solvents.

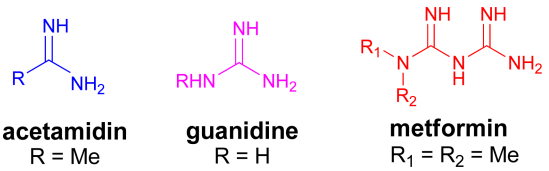

Scheme 1. Structures of amidines, guanidines and biguanides.

Experimental

Reagents. $FeCl_2{\cdot}4H_2O$, $FeCl_3{\cdot}6H_2O$, ammonium hydroxide (28% NH_3 in water), hydrochloric acid (37%), tetraethylorthosilicate (TEOS), 3-chloropropyl-trimethoxysilane (CPTS), trisodium citrate, benzaldehydes, malononitrile, K_2CO_3, KI and solvents were purchased all from Merck. Benzaldehyde and 2-furaldehyde were distilled before used and metformin hydrochloride was purchased from Aldrich.

Characterization. TEM measurements were performed using a Philips CM10 operated at 100 kV electron beam accelerating voltage and equipped with a CCD camera. One drop of the sample solution was deposited onto a copper grid and the excess of the droplet was blotted off the grids with filter paper; then the sample was dried under ambient conditions. The sizes of the magnetic nanoparticle cores were determined by photoenlarging the micrographs and measuring at least 40 individual cores manually.

The XRD patterns of samples were recorded on a D8 Advanced diffractometer (Bruker AXS Inc., 40 kV, 30 mA) X-ray diffractometer. Scans were taken with a 2θ and step size of 0.02 from 3 to 70° and a counting time of 1.0 s using a Cu Kα radiation source (λ = 1.542 Å) and a nickel filter. The specific surface area (BET method), the total pore volume and the mean pore diameter (BJH method) were measured using a N_2 adsorption-desorption isotherm by using a NOVA 2200 instrument. Thermogravimetric analyses were performed on a NETZSCH TG 209 F1 Iris analyzer. TGA measurements were carried out with a dynamic temperature program of 25-800 °C with a heating rate 10 °C/min. Carbon, hydrogen, and nitrogen contents was determined with a EuroEA3000 CHNS-O elemental analyzer (EuroVector S.p.A., Italy). The magnetic measurements were carried out in a vibrating sample magnetometer (VSM, BHV-55, Riken, Japan) at room temperature. Infrared spectra were prepared on a Ray Leigh Wqf-510 FT-IR spectrophotometer. NMR spectra were recorded on a Brucker Avance spectrophotometer (200 MHz) in $CDCl_3$ and DMSO-d_6 using TMS as an internal standard.

Synthesis and Modification of Magnetic Nanoparticles (Fe_3O_4). Iron oxide magnetic nanoparticles (MNPs) modified with citrate groups were prepared according to a reported procedure by Yang *et al*.[13] Typically, iron (III) chloride hexahydrate (2.70 g, 10 mmol) and iron (II) chloride tetrahydrate (1 g, 5 mmol) were dissolved in distilled water (130 mL) in Ar atmosphere. Then, 11 mL of ammonium hydroxide 28% was quickly added into the solution under rapid mechanical stirring (900 rpm), and then the mixture was heated up to 60 °C, while vigorously stirred by a mechanical stirrer for 1 hr under argon. Finally, after cooling to room temperature, the resultant nanoparticles were collected using a magnet and the collected magnetic solid were dispersed in a 200 mL of trisodium citrate solution (0.3 M) and heated at 80 °C for 1 h. Then, the precipitates were collected using an external magnet and washed with acetone to remove remnant trisodium citrate.

Synthesis of Silica-Coated MNPs (Fe_3O_4/SiO_2). Following the Stöber method with some modifications,[14] the surface modified MNPs (1 g) were redispersed in 50 mL of distilled water by the ultrasonic treatment for 20 min to form a ferro fluid. Subsequently, the resultant dispersion was centrifuged for 30 min and adjusted to 2.0 wt %. 2 mL of the ferro fluid was first diluted with water (40 mL), the resultant suspension and 5 mL of $NH_3.H_2O$ were poured into 140 mL of ethanol with vigorous stirring at 40 °C. Finally, under continuous mechanical stirring, 1 mL of TEOS diluted in ethanol (20 mL) was dropwise added to this dispersion. The resulting dispersion was kept stirred mechanically for 14 h at room temperature. The magnetic Fe_3O_4/SiO_2 nanoparticles were collected by magnetic separation and washed with ethanol and deionized water in sequence.

Synthesis of Metformin-Modified Silica-Coated MNPs (Fe_3O_4/SiO_2-Met). First, chloropropyl-modified silica-coated magnetic nanoparticles were prepared following the modified procedure of Zeng *et al.*[15] After 1 mL (5 mmol) of CPTS was dissolved in 100 mL of dried toluene, this mixture was added to 1 g of Fe_3O_4/SiO_2 and the solution was stirred for 18 h at 60 °C. The chloropropyl-functionalized solid (Fe_3O_4/SiO_2-Cl) was washed with toluene, separated by a magnet, and dried in vacuum. The obtained magnetic solid was used in the following step to synthesize metformin-modified silica-coated MNPs. The prepared Fe_3O_4/SiO_2-Cl (1 g) and KI (1.66 g, 10 mmol) were added to a solution of metformin hydrochloride (0.21 g, 5 mmol) and K_2CO_3 (10 mmol, 1.38 g) in acetonitrile (50 mL) in a round-bottom flask and the mixture was stirred under reflux condition for 5 hrs. The obtained solid was then magnetically collected from the solution and washed copiously with water/ethanol followed by drying at 80 °C for 6 hrs.

Catalytic Study.

The Nitroaldol Reaction: The nitroaldol (Henry) reaction was performed by mixing 2-furaldehyde (96 mg, 1 mmol), nitromethane (122 mg, 2 mmol), catalyst (50 mg) and EtOH (10 mL), in a 25 mL round-bottom flask, and stirring the mixture for 8 h at room temperature. The catalyst was easily separated from the reaction mixture by a magnet and the residual solution was concentrated in vacuum to afford the crude product, which was further analyzed by ^{1}H NMR in $CDCl_3$.

Preparation of Pyrano[3,2-*c*]chromenes and Tetrahydro-4*H*-chromenes: A mixture of an aromatic aldehyde (1 mmol), malononitrile (1 mmol), 4-hydroxycoumarin or dimedone (1 mmol) and 30 mg of Fe_3O_4/SiO_2-Met in EtOH/H_2O (1:1) was stirred at reflux for 1 h. After completion of the reaction, the catalyst was easily separated by a magnet and the solid product was purified by recrystallization from ethanol.

Selected Spectroscopic Data.

2-Amino-4-(phenyl)-3-cyano-4*H*,5*H*-pyrano[3,2-*c*] chromene-5-one (Compound 3a): mp 259 °C (lit.,[16] 256-258 °C), ν_{max}/cm^{-1} (KBr): 3373, 3281, 3168, 2189, 1705,1669, 1602. ^{1}H NMR (DMSO-d_6, 200 MHz) δ 4.44 (s,1H), 7.25 (d, *J* = 7.8 Hz, 2H), 7.29 (br s, 1H), 7.33 (t, *J* = 7.5 Hz, 2H), 7.42 (br s, 2H), 7.46 (d, *J* = 8. 4 Hz, 1H), 7.48 (t, *J* = 7.6 Hz, 1H), 7.69 (t, *J* = 7.5 Hz, 1H), 7.89 (d, *J* = 7.8 Hz, 1H). ^{13}C NMR (DMSO-d_6, 50 MHz) δ 58.9, 104.9, 113.7, 117.3, 120.2, 123.3, 125.4, 128.0, 128.6, 129.4, 133.8, 144.2, 153.1, 154.3, 158.9, 160.3.

2-Amino-4-(4-chlorophenyl)-3-cyano-4*H*,5*H*-pyrano-[3,2-*c*] chromene-5-one (Compound 3b): mp 260 °C (lit.,[16] 263-265°C), ν_{max}/cm^{-1} (KBr): 3385, 3318, 3192, 2189, 1712, 1671, 1606. ^{1}H NMR (DMSO-d_6, 200 MHz) δ 4.48 (s, 1H), 7.31 (d, *J* = 8.2 Hz, 2H), 7.35 (br s, 2H), 7.37 (br s, 2H),

7.45 (d, J = 8.2 Hz, 1H), 7.48 (t, J = 7.6 Hz, 1H), 7.68 (t, J = 7.8 Hz, 1H), 7.94 (d, J = 7.8 Hz, 1H). ^{13}C NMR (DMSO-d_6, 50 MHz) δ 58.6, 104.3, 113.7, 117.4, 119.9, 123.4, 125.42, 129.28, 130.45, 132.65, 133.75, 143.12, 153.06, 154.4, 159.0, 160.4.

2-Amino-4-(2,4-dichlorophenyl)-3-cyano-4*H*,5*H*-pyrano-[3,2-*c*] chromene-5-one (Compound 3c): mp 254 °C (lit.,[16] 257-259 °C), ν_{max}/cm^{-1} (KBr): 3461, 3293, 3161, 3072, 2194, 1715, 1670, 1588. ^{1}H NMR (DMSO-d_6, 200 MHz) δ 4.98 (s, 1H), 7.36 (dd, J = 8.3, 1.9 Hz, 1H), 7.41 (d, J = 8.3 Hz, 1H), 7.42 (br s, 2H), 7.46 (d, J = 8.3 Hz, 1H), 7.52 (t, J = 7.7 Hz, 1H), 7.57 (d, J = 2.1 Hz, 1H), 7.74 (t, J = 8.2 Hz, 1H), 7.91 (d, J = 8.9 Hz, 1H). ^{13}C NMR (DMSO-d_6, 50 MHz) δ 57.2, 103.4, 113.8, 117.5, 119.6, 123.5, 125.6, 128.8, 129.8, 132.9, 133.4, 133.9, 134.3, 140.3, 153.2, 155.1, 159.2, 160.4.

Amino-4-(4-nitrophenyl)-3-cyano-4*H*,5*H*-pyrano[3,2-*c*] chromene-5-(Compound 3d): mp 261 °C (lit.,[16] 258-260 °C), ν_{max}/cm^{-1} (KBr): 3478, 3428, 3375, 3337, 2190, 1717, 1670, 1607, 1504, 1372, 1306. ^{1}H NMR (DMSO-d_6, 200 MHz) δ 4.68 (s, 1H), 7.43 (d, J = 8.3 Hz, 1H), 7.50 (t, J = 7.7 Hz, 1H), 7.57 (br s, 2H), 7.60 (d, J = 8.0 Hz, 2H), 7.73 (t, J = 7.8 Hz, 1H), 7.85 (d, J = 7.8 Hz, 1H), 8.18 (d, J = 8.3 Hz, 2H). ^{13}C NMR (DMSO-d_6, 50 MHz) δ 57.6, 103.6, 113.8, 117.45, 119.9, 123.5, 124.6, 125.4, 130.1, 134.1, 147.4, 151.6, 153.2, 154.8, 158.9, 160.4.

2-Amino-7,7-dimethyl-5-oxo-4-phenyl-5,6,7,8-tetrahydro-4*H*-chromene-3-carbonitrile (Compound 4a): mp 227 °C (lit.,[17] 226-228 °C), ν_{max}/cm^{-1} (KBr): 3394, 3325, 2199, 1676, 1215. ^{1}H NMR (DMSO-d_6, 200 MHz) δ 1.07 (s, 3H), 1.11 (s, 3H), 2.15 (H-6b, J_{AB} = 16 Hz), 2.26 (H-6a, J_{AB} = 16 Hz), 2.46 (s, 2H), 4.33 (s, 1H), 5.85 (s, 2H), 7.11-7.32 (m, 5H). ^{13}C NMR (DMSO-d_6, 50 MHz) δ 26.7, 28.4, 31.7, 35.5, 39.5, 50.2, 58.5, 113.1, 119.2, 126.6, 127.3, 128.2, 144.6, 158.5, 162.3, 195.5

2-Amino-4-(4-methoxyphenyl)-7,7-dimethyl-5-oxo-5,6,7,8-tetrahydro-4*H*-chromene-3-carbonitrile (Compound 4b): mp 195 °C (lit.,[17] 197-199 °C), ν_{max}/cm^{-1} (KBr): 3378, 3327, 2198, 1683, 1213. ^{1}H NMR (DMSO-d_6, 200 MHz) δ 1.05 (s, 3H), 1.1 (s, 3H), 2.16 (H-6b, J_{AB} = 16 Hz), 2.24 (H-6a, J_{AB} = 16 Hz), 2.45 (s, 2H), 3.75 (s, 3H), 4.34 (s, 1H), 5.63 (s, 2H), 6.82 (d, J = 8.6 Hz, 2H), 7.12 (d, J = 8.6 Hz, 2H), ^{13}C NMR (DMSO-d_6, 50 MHz) δ 26.7, 28.4, 32.6, 34.6, 40.6, 50.1, 55.1, 58.6, 113.0, 113.8, 119.6, 128.1, 136.6, 157.7, 158.3, 162.5, 195.4.

2-Amino-7,7-dimethyl-4-(4-nitrophenyl)-5-oxo-5,6,7,8-tetrahydro-4*H*-chromene-3-carbonitrile (Compound 4c): mp 173 °C (lit.,[17] 175-176 °C), ν_{max}/cm^{-1} (KBr): 3510, 3369, 2182, 1683, 1214. ^{1}H NMR (DMSO-d_6, 200 MHz) δ 1.03 (s, 3H), 1.10 (s, 3H), 2.18 (H-6b, J_{AB} = 16 Hz), 2.27 (H-6a, J_{AB} = 16 Hz), 2.48 (s, 2H), 4.33 (s, 1H), 5.97 (s, 2H), 7.38 (d, J = 8.7 Hz, 2H), 8.2 (d, J = 8.7 Hz, 2H), ^{13}C NMR (DMSO-d_6, 50 MHz) δ 27.4, 28.2, 31.7, 35.6, 39.6, 49.8, 57.2, 112.1, 119.3, 123.6, 128.7, 146.1, 152.2, 158.4,163.1, 195.5.

2-Amino-7,7-dimethyl-4-(3-nitrophenyl)-5-oxo-5,6,7,8-tetrahydro-4*H*-chromene-3-carbonitrile (Compound 4d): mp 206 °C (lit.,[17] 201-205 °C), ν_{max}/cm^{-1} (KBr): 3433, 3335, 2178, 1668, 1217. ^{1}H NMR (DMSO-d_6, 200 MHz) δ 1.03 (s, 3H), 1.1 (s, 3H), 2.17 (H-6b, J_{AB} = 16 Hz), 2.25 (H-6a, J_{AB} = 16 Hz), 2.50 (s, 2H), 4.47 (s, 1H), 6.32 (s, 2H), 7.47-7.51 (m, 1H), 7.63-7.66 (m, 1H), 8.03-8.05 (m, 2H), ^{13}C NMR (DMSO-d_6, 50 MHz) δ 26.8, 28.3, 32.3, 35.3, 39.5, 49.7, 58.7, 118.3, 119.2, 120.8, 125.6, 130.3, 136.5, 143.4, 150.6, 157.4, 163.4, 196.5.

General Procedure for Recycling Experiments. The reusability of the catalyst was studied taking 50 mg of the Fe_3O_4/SiO_2-Met catalyst in recycling experiments. In order to regenerate the catalyst, at the end of the reaction, it was separated by simple magnetic decantation using a permanent magnet. Then the catalyst was washed repeated with ethyl acetate and reused in the next reaction with a fresh reaction mixture for several times.

Results and Discussion

The schematic pathways for preparing the metformin-modified silica-coated MNPs are depicted in Scheme 2. First, the chemical co-precipitation of Fe^{2+} and Fe^{3+} ions in basic solution led to the formation of magnetite nanoparticles. By virtue of the modification of magnetite nanoparticles with citrate groups, highly stable magnetic fluid containing well-dispersed magnetite nanoparticles can be obtained Yang *et al.*[13] Then, in order to avoid possible aggregation or oxidation of the iron oxide nanoparticles, a layer of SiO_2 was coated on the nanoparticles as the iron oxide surface has a strong affinity for silica. This was achieved using the modified Stöber method resulting in the formation of stable silica shell on the Fe_3O_4 surface.[13,14]

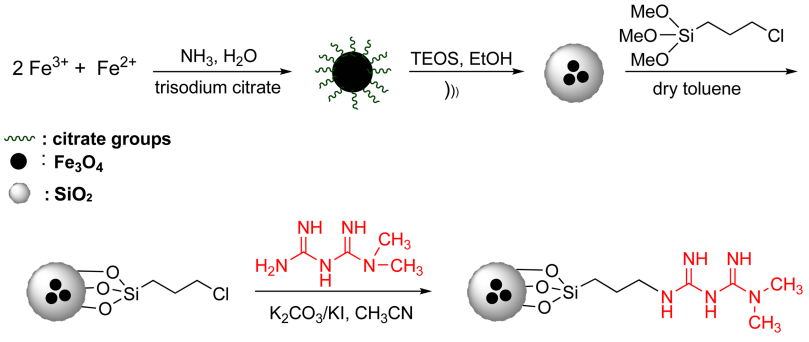

Scheme 2. Preparation of Fe_3O_4/SiO_2-Met nanoparticles.

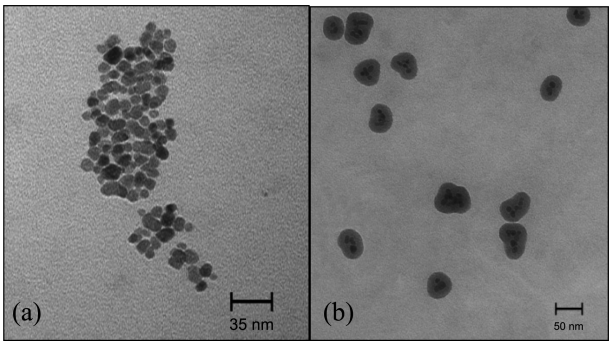

Figure 1. TEM images of solutions containing (a) monodispersed Fe_3O_4 nanoparticles treated with trisodium citrate and (b) core-shell Fe_3O_4/SiO_2 nanoparticles.

The morphology of MNPs before and after silica coating was studied by transmission electron microscopy (TEM) by drop casting suspensions in H_2O onto carbon-coated copper grids shown in Figure 1. The TEM observation indicates that the trisodium citrate-treated magnetite nanoparticles are monodispersed and have average diameter ranging about 9.2 nm (Fig. 1(a)). Furthermore, Figure 1(b) shows that the silica-modification process of MNPs leads to the formation of magnetic/silica composite particles with typical core-shell structure. These observations confirmed the formation of a silica layer around the Fe_3O_4 nanoparticles.

Additionally, the crystalline structure of Fe_3O_4 nanoparticles before and after silica coating, were identified with XRD technique (Fig. 2). For citrate-coated Fe_3O_4, diffraction peaks with 2θ at 30.4°, 35.6°, 43.3°, 53.7°, 57.3°, and 62.8°, indicative of a cubic spinel structure of the magnetite were observed which conforms well to the reported value (JCPDS no. 65-3107), implying the formation of a Fe_3O_4 phase.[18] The (311) XRD peak was used to estimate the mean nanoparticle diameter by Scherrer's formula $D = 0.9\lambda/\beta \cos\theta$, where D is the average crystalline size, λ is the X-ray wavelength (1.542 Å), β is the angular linewidth of half-maximum intensity and θ is Bragg's angle in degree.[19] The mean crystallite size calculated using this formula is about 9.5 nm, consistent with the result measured from the TEM images (Fig. 2(a)). After silica-coating process, it is seen that no change is occurred in the crystalline structure of the Fe_3O_4 core and only intensity of the related peaks of silica-coated Fe_3O_4 nanoparticles are slightly reduced. This is mainly due to the formation of an amorphous silica shell around the Fe_3O_4 core.[13] The presence of a broad peak at 20°-28° is in a good agreement with the amorphous structure of silica layer.

For the attachment of biguanide to the surface of silica-coated Fe_3O_4 nanoparticles through a covalent bond linkage, first, the surface of Fe_3O_4/SiO_2 was modified with 3-chloropropyl-trimethoxysilane (CPTS) as a spacer. This modification was performed according to the known reaction sequence.[15] Then, biguanide-modified Fe_3O_4/SiO_2 was prepared by the reaction of metformin with chloropropyl-grafted Fe_3O_4/SiO_2 and the success of this immobilization was monitored with various techniques.

Successful silica-coating and subsequent biguanide functionalization of the Fe_3O_4 nanoparticles can be inferred from FT-IR techniques. Figure 3(a) shows the FT-IR spectrum of Fe_3O_4 modified with trisodium citrate and its band characteristics. The signal observed at 579 cm^{-1} is attributed to the Fe-O bond vibration.[20] In addition, two bands observed at 1617 and 1385 cm^{-1}, which are due to the COO-Fe bond and confirm the complexation between the carboxylate moiety of citrate groups and iron ions on the magnetite nanoparticles surface.[13] In the case of Fe_3O_4/SiO_2 nanoparticles (curve b), the sharp band at 1090 cm^{-1} is corresponding to Si-O-Si anti-symmetric stretching vibration, being indicative of the existence of a SiO_2 layer around the Fe_3O_4 nanoparticles.[21] Biguanides like guanidines absorb strongly around 1570 cm^{-1} due to C=N stretching vibrations[22] and spectrum of the metformin-modified nanoparticles (curve c) shows a band appeared at 1568 that is attributed to the presence of biguanide functionality. Although, the signals appeared at 3200-3500 cm^{-1} region can be assigned to the water in atmosphere, but we believe that the signal observed at 3383 cm^{-1} is attributed to the N-H stretching of C=N-H group on metformin.[22] All together, the aforementioned results confirmed the formation of a silica layer around the Fe_3O_4 nanoparticles and the biguanide-functionalization of this core-shell structure.

The measured BET surface areas are 123.7, 174.3 and 153.8 m^2/g for trisodium citrate-treated Fe_3O_4, Fe_3O_4/SiO_2, and Fe_3O_4/SiO_2-Met nanoparticles, respectively (listed in

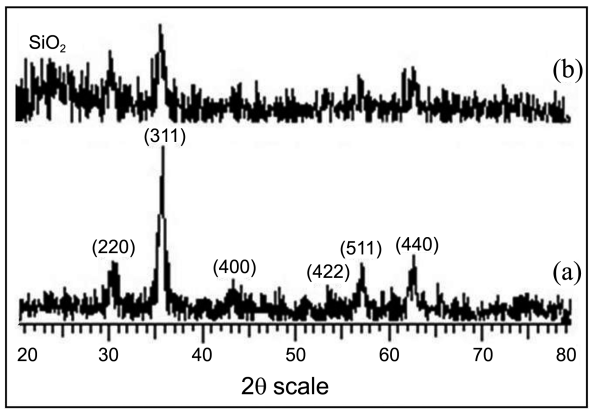

Figure 2. XRD diffractograms for (a) trisodium citrate-treated magnetite nanoparticles and (b) silica-coated Fe_3O_4 nanoparticles.

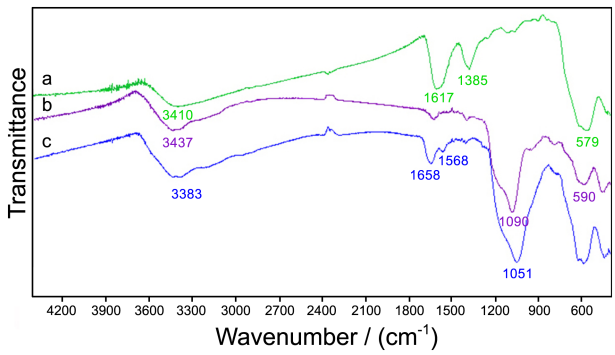

Figure 3. FT-IR spectra of (a) trisodium citrate-treated magnetite nanoparticles, (b) Fe_3O_4/SiO_2 and (c) Fe_3O_4/SiO_2-Met.

Table 1. Characterization of trisodium citrate-treated Fe_3O_4, Fe_3O_4/SiO_2 and Fe_3O_4/SiO_2-Met by N_2 adsorption-desorption measurement

Sample	BET surface area (m^2/g)	BJH Pore Volume Cm^3/g
Fe_3O_4	123.7	7.63 E^{-02}
Fe_3O_4/SiO_2	174.3	8.36 E^{-02}
Fe_3O_4/SiO_2-Met	153.8	6.02 E^{-02}

Table 1) and corresponded pore volumes are 0.0763, 0.0836, 0.0602 cm^3/g respectively obtained from analysis of the desorption using the BJH (Barett-Joyner-Halenda) method. The results show that after coating of Fe_3O_4 with SiO_2, specific surface area and pores volume increase due to the low specific weight of silica compared to that of magnetite. The specific surface area and pore volume for Fe_3O_4/SiO_2-Met decreases, that is due to the blockage of the pores of Fe_3O_4/SiO_2 with metformine-ended chains confined on the surface of Fe_3O_4/SiO_2.[23]

Elemental analysis results showed that the carbon, hydrogen, and nitrogen content of Fe_3O_4/SiO_2-Met nanoparticles was 3.218, 0.627, and 1.048 (wt %), respectively, equivalent to a loading of ~0.15 mmol of biguanide groups per gram of nanoparticles, indicative of the successful functionalization of biguanidylpropyl groups.

TGA analyses of the nanoparticles were also used to determine the percent of organic functional groups chemisorbed onto the surface of Fe_3O_4/SiO_2-Met. Figure 4 curves a and b represents the TGA of Fe_3O_4/SiO_2 and as-prepared Fe_3O_4/SiO_2-Met, respectively. In both cases, the weight loss at temperatures below 200 ºC can be attributed to the water desorption from the surface of silica layer and weight loss above 600 ºC is associated with the release of the structure water.[24,25] Furthermore, curve b shows a weight loss (6.91 wt %) from 200 to 600 ºC apart from two water loss events, resulting from the decomposition of biguanidylpropyl groups grafted to the silica surface. These results prove that the attachment of biguanide moiety onto the surface of Fe_3O_4/SiO_2 nanoparticle.

The magnetic property of Fe_3O_4/SiO_2 nanoparticle was characterized by a vibrating sample magnetometer (VSM) and Figure 5 shows the typical room temperature magnetization curve of Fe_3O_4/SiO_2. It is reported that the *M*s (saturation magnetization) of bare Fe_3O_4 nanoparticles is 73.7 emu/g[26] and the *M*s of the Fe_3O_4/SiO_2-Met nanocatalyst prepared in this study is 46.7 emu/g. The nearly lower saturation magnetization of the nanocatalyst, compared to that of bare Fe_3O_4 nanoparticles, can be attributed to the formation of a silica shell around the Fe_3O_4 core. It has been reported that the Fe_3O_4 nanoparticles with a high value of coercivity (*Hc*) could be called ferromagnetic at room temperature, whereas those with a low value (lower than 20 Oe) could be called superparamagnetic. Our results showed that the *Hc* of catalyst is 1.13 Oe and the *Mr* (remanent magnetization) is ~0.15 emu/g. As a result, the synthesized nanocatalysts in this study had a typical superparamagnetic behavior[27,28,29] and thus, they could be readily and stably dispersed in water and remained in suspension in the absence of external magnetic.

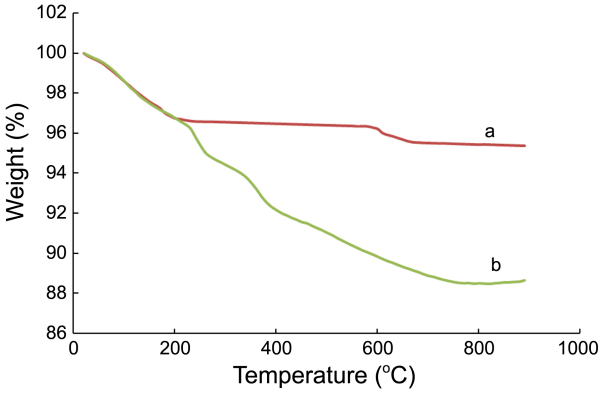

Figure 4. TGA curves of (a) Fe_3O_4/SiO_2, (b) Fe_3O_4/SiO_2-Met.

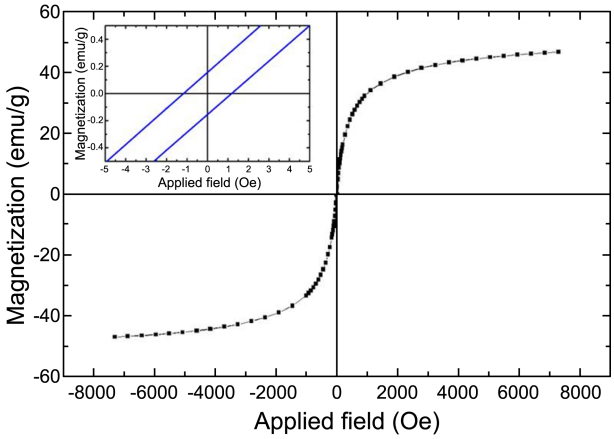

Figure 5. Hysteresis loop of the Fe_3O_4/SiO_2-Met nanoparticle at room temperature. Left inset: the magnified field from −5 to 5 Oe.

The catalytic ability of the magnetite nanoparticle-supported biguanide catalyst was evaluated in catalyzing a series of various organic transformations like nitroaldol C-C coupling reaction of 2-furaldehyde with C-H acid (nitromethane, Table 2) and domino Knoevenagel condensation/Michael addition/cyclization reactions (Table 3).

Table 2. The Henry reaction between 2-furaldehyde and nitromethane in room temperature

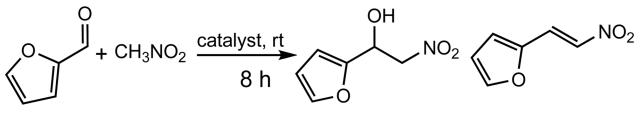

Entry	Catalysts	Conv. (%)	NMR yield (%)	
			A	B
1	Fe_3O_4/SiO_2	0	-	-
2	Fe_3O_4/SiO_2/NH_2 (30 mg)	40	0	40
3	Fe_3O_4/SiO_2/Met (30 mg)	45	45	0
4	Fe_3O_4/SiO_2/Met (50 mg)	65	65	0
5	Fe_3O_4/SiO_2/Met (15 mg)	20	20	0

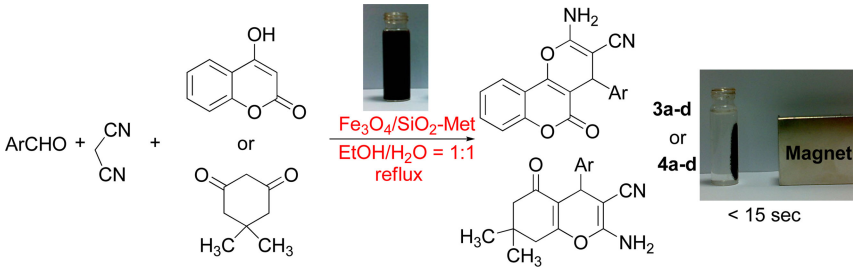

Scheme 3. Catalytic performance of Fe_3O_4/SiO_2-Met for the one-pot synthesis 2-amino-4-aryl-3-cyano-5-oxo 4*H*,5*H*-pyrano-[3,2-*c*]chromenes and tetrahydrobenzo[*b*]pyran.

In the case of nitroaldol reaction, the initial reaction was carried out using of catalyst ranging from 0-50 mg at room temperature in EtOH as the solvent. The results were evaluated qualitatively through TLC. It was found that the quantitative yield can be achieved when the reaction was carried out in the presence of 50 mg catalyst at rt for 8 h in EtOH. The further studies showed that the use of unmodified Fe_3O_4/SiO_2 system caused no conversion (Table 2, entry 1) while the use of Fe_3O_4/SiO_2/Met (50 mg) led to a chemoselective formation of the product A in 65% yield (Table 2, entry 4). Interestingly, the aminopropyl-functionalized catalyst $Fe_3O_4/SiO_2/NH_2$ led to the chemoselective formation of product B which is formed upon dehydration of product A. (Table 2, entry 2). These results suggest that Fe_3O_4/SiO_2/Met is more suitable for this reaction due to its stronger basicity as well as several amine sites.

The catalytic performance of the metformin-functionalized magnetite nanoparticles was also evaluated in domino Knoevenagel condensation/Michael addition/cyclization reaction for the preparation of 2-amino-4-aryl 3-cyano-5-oxo-4*H*,5*H*-pyrano-[3,2-*c*] chromenes derivatives[16] by condensing 4-hydroxycoumarin, aldehydes and malononitriles using 30 mg of Fe_3O_4/SiO_2-Met in medium H_2O:EtOH (1:1) at reflux.

Furthermore, the three-component reaction of dimedone, aldehydes and malononitrile for preparation of tetrahydrobenzo[*b*] pyrans was examined (Scheme 3, Table 3).[17] The synthesized compounds in this project were all known and easily identified by comparison of their spectroscopic data with those reported in literature (refs in Table 3).

Table 3. One-pot synthesis of 2-amino-4-aryl-3-cyano-5-oxo-4*H*,5*H*-pyrano-[3,2-*c*]chromenes and tetrahydrobenzo[*b*]pyran catalyzed by biguanide-functionalized magnetite nanoparticles[a]

Entry	Substrate	Product	Yield[b]	mp (Lit. mp °C)[ref]
1	C_6H_5	**3a**	85	259 (256-258)[16]
2	4-ClC_6H_4	**3b**	86	260 (263-265)[16]
3	2,4-$Cl_2C_6H_3$	**3c**	84	254 (257-259)[16]
4	4-$NO_2C_6H_4$	**3d**	94	261 (258-260)[16]
5	C_6H_5	**4a**	86	227 (226-228)[17]
6	4-$CH_3OC_6H_4$	**4b**	86	195 (197-199)[17]
7	4-$NO_2C_6H_4$	**4c**	92	173 (175-176)[17]
8	3-$NO_2C_6H_4$	**4d**	78	206 (201-205)[17]

[a]Combination of the reagents: Nanocatalyst (30 mg), aldehyde 1 mmol, malononitrile 1 mmol, (4-hydroxycoumarin or dimedone) 1 mmol, H_2O:EtOH (1:1) 10 mL for 1h at reflux. [b]Yields of the isolated products.

Finally, to assess the catalytic capability of the prepared catalyst with respect to the reported ones for catalyzing nitroaldol C-C coupling and domino Knoevenagel condensation/Michael addition/cyclization reactions, synthesis of the desired products utilizing Fe_3O_4/SiO_2-Met was compared with some of the reported catalysts such as cyclen, S-proline, $H_6P_2W_{18}O_{62}\cdot 18H_2O$, $Yb(PFO)_3$, free metformine and *etc.* (Table 4). As is clear from Table 4, the present procedure involving avoidance of organic volatile solvents and toxic catalysts, mild condition and the use of a recoverable and cost-effective magnetic catalyst is very simple and convenient. In general, the reactions were very clean and high yielding and they proceed without introducing any acid, base

Table 4. Comparison of the literature results for the preparation of **A**, **3b** and **4d** with the result using this method

Entry	Catalyst	Conditions	Product	Yield	Time
1	Triethylamine (1 mmol)	H_2O, rt	**A**	45	6.5 h[30]
2	Cyclen (10 mol %)	THF, 5 °C under argon.	**A**	55	24 h[31]
3	Metformine (10 mol %)	EtOH, rt	**A**	75	12 h
4	Fe_3O_4/SiO_2/Met (50 mg)	EtOH. rt	**A**	65	8 h
5	*S*-proline (10 mol %)	H_2O:EtOH (1:1), reflux	**3b**	78	2 h[32]
6	$H_6P_2W_{18}O_{62}\cdot 18H_2O$, (1 mol %)	H_2O:EtOH (1:1), reflux	**3b**	89	75 min[33]
7	Fe_3O_4/SiO_2/Met (30 mg)	H_2O:EtOH (1:1), reflux	**3b**	86	1 h
8	Fe_3O_4/SiO_2/Met (15 mg)	H_2O:EtOH (1:1), reflux	**3b**	55	1h
9	$Yb(PFO)_3$ (5 mol %)	EtOH, 60 °C	**4d**	83	4 h[34]
10	Na_2SeO_4	H_2O:EtOH (1:1), reflux	**4d**	90	2.5 h[35]
11	Fe_3O_4/SiO_2/Met (30 mg)	H_2O:EtOH (1:1), reflux	**4d**	78	1 h

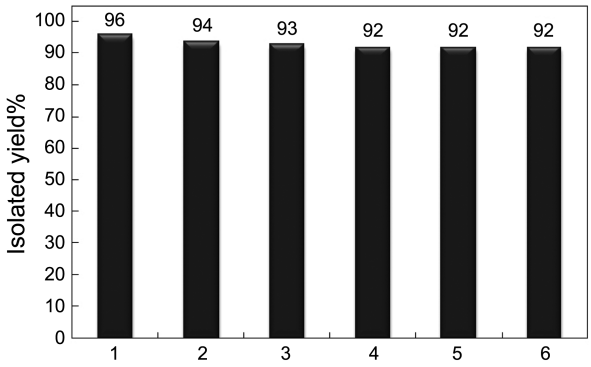

Figure 6. The recycling of the Fe_3O_4/SiO_2-Met (50 mg) carried out under reflux conditions for 1 h using a model reaction of 4-nitrobenzaldehde, malononitrile and 4-hydroxycoumarin.

or metal catalyst and also no side products were detected in any reaction.

Surprisingly, at the end of each reaction, the nanoparticles were easily separated with an external magnet and the recovered catalyst was reused for at least six runs without significant degradation in catalytic activity and performance (Fig. 6).

Conclusion

In summary, a novel superbase (biguanide)-functionalized magnetite nanoparticle has been synthesized through the facile and simple synthetic procedures starting from commercially available starting materials. After structural characterization of the synthesized nano-based catalyst, its capability in promoting the organic transformations was investigated in some details. It was found that the biguanide-functionalized magnetite nanoparticle can be utilized as efficient heterogeneous catalyst for the nitroaldol and sequential reactions under mild conditions showed excellent stability, activity and reusability. Also notably, recovery of the catalyst can be achieved easily with the help of an external magnet in a very short time (< 15 seconds) with no need for expensive ultracentrifugation. The recyclability of the catalyst was also investigated and it was observed that even after several times use of the catalyst in a number of transformations, it is stable enough and can be used several times with no loss in activity.

Acknowledgments. We are grateful to the University of Razi Research Council for the partial support of this work. M. Beygzadeh is also thankful to the Iran Nanotechnology Initiative Council (INIC) for their partial support on this project.

References

1. Ishigawa, T. *Superbases for Organic Synthesis: Guanidines, Amidines, Phosphazenes and Related Organocatalysts*; John Wiley & Sons: 2009.
2. Haflinger, G.; Kuske, F. K. H. *The Chemistry of Amidines and Imidates*; John Wiley & Sons: Chichester, 1991.
3. Gladysz, J. A. *Chem. Rev.* **2002**, *102*, 3215.
4. Leadbeater, N. E.; Marco, M. *Chem. Rev.* **2002**, *102*, 3217.
5. Hu, A.; Yee, G. T.; Lin, W. *J. Am. Chem. Soc*. **2005**, *127*, 12486.
6. Shylesh, S.; Schunemann, V.; Thiel, W. R. *Angew. Chem. Int. Ed*. **2010**, *49*, 3428.
7. Ranganath, K. V. S.; Glorius, F. *Catal. Sci. Technol*. **2011**, *1*, 13.
8. Polshettiwar, V.; Luque, R.; Fihri, A.; Zhu, H.; Bouhrara, M.; Basset, J. M. *Chem. Rev.* **2011**, *111*, 3036.
9. Macquarrie, D. J.; Jackson, D. B.; Tailland, S.; Utting, K. A. *J. Mater. Chem*. **2001**, *11*, 1843.
10. Kim, K. S.; Somg, J. H.; Kim, J. H.; Seo, G. *Stud. Surf. Sci. Catal*. **2003**, *146*, 505.
11. Phan, N. T. S.; Jones, C. W. *J. Mol. Catal. A* **2006**, *253*, 123.
12. Gelbard, G.; Vielfaure-Joly, F. *Tetrahedron Lett*. **1998**, *39*, 2743.
13. Yang, D.; Hu, J.; Fu, S. *J. Phys. Chem. C* **2009**, *113*, 7646.
14. Stober, W.; Fink, A.; Bohn, E. J. *J. Colloid Interface Sci.* **1968**, *26*, 62.
15. Zeng, T.; Yang, L.; Hudson, R.; Song, G.; Moores, A.-R.; Li, C.-J. *Org. Lett.* **2011**, *13*, 442.
16. Abdolmohammadi, S.; Balalaie, S. *Tetrahedron Lett*. **2007**, *48*, 3299.
17. Kumar, D.; Reddy, V. B.; Sharad, S.; Dube, U.; Kapur, S. *Eur. J. Med. Chem*. **2009**, *44*, 3805.
18. Yang, T. Z.; Shen, C. M.; Gao, H. J. *J. Phys. Chem. B* **2005**, *109*, 23233.
19. Giri, J.; Thakurta, S. G.; Bellare, J.; Nigam, A. K.; Bahadur, D. *J. Magn. Magn. Mater.* **2005**, *293*, 62.
20. Waldron, R. D. *Phys. Rev.* **1955**, *99*, 1727.
21. Yamaura, M.; Camiloa, R. L.; Sampaio, L. C.; Macedo, M. A.; Nakamura, M.; Toma, H. E. *J. Magn. Magn. Mater*. **2004**, *279*, 210.
22. Gunasekaran, S.; Natarajan, R. K.; Renganayaki, V.; Natarajan, S. *Indian. J. Pure & Applied Physics* **2006**, *44*, 495.
23. Wang, J.; Zheng, S.; Shao, Y.; Liu, J.; Xu, Z.; Zhu, D. *J. Colloid Interface Sci.* **2010**, *349*, 293.
24. Lei, Z.; Li, Y.; Wei, X. *J. Solid State Chem*. **2008**, *181*, 480.
25. Chang, Y. C.; Chen, D. H. *J. Colloid Interface Sci*. **2005**, *283*, 446.
26. Naka, K.; Narital, A.; Tanakal, H.; Chujo, Y.; Morita, M.; Inubushi, T.; Nishimura, I.; Hiruta, J.; Shibayama, H.; Koga, M.; Ishibashi, S.; Seki, J.; Kizaka-Kondoh, S.; Hiraoka, M. *Polym. Adv. Technol*. **2008**, *19*, 1421.
27. Ohandley, R. C. *Modern Magnetic Materials: Principles and Applicat Ions*; Wiley: New York, 2000.
28. Iida, R. H.; Takayanagi, K.; Nakanishi, T.; Osaka, T. *J. Colloid Interface Sci*. **2007**, *314*, 274.
29. ChengLin, G. W.; Huan, H.; HongJun, G.; Gan, L.; RuJiang, M.; YingLi, A.; LinQi, S. *Sci. China Chem.* **2010**, *53*, 514.
30. Zhou, C. L.; Zhou, Y. Q.; Wang, Z. Y. *Chinese Chem. Lett.* **2003**, *14*, 355.
31. Bray, C. V.; Jiang, F.; Wu, X. F.; Sortais, J.-B.; Darcel, C. *Tetrahedron Lett*. **2010**, *51*, 4555.
32. Abdolmohammadi, S.; Balalaie, S. *Tetrahedron Lett*. **2007**, *48*, 3299.
33. Heravi, M. M.; Alimadadi-Jani, B.; Derikvand, F.; Bamoharram, F. F.; Oskooie, H. A. *Catal. Commun.* **2008**, *10*, 272.
34. Wang, L. M.; Shao, J. H.; Tian, H.; Wang, Y. H.; Liu, B. *J. Fluorine Chem*. **2006**, *127*, 97.
35. Hekmatshoar, R.; Majedi, S.; Bakhtiari, K. *Catal. Commun.* **2008**, *9*, 307.